

Ivan Franko National University of Lviv

IEEE Ukraine Section

IEEE Ukraine Section (West) MTT/ED/AP/EP/SSC Societies Joint Chapter



2019

**XIth International Scientific and Practical Conference on
ELECTRONICS AND INFORMATION
TECHNOLOGIES
(ELIT)**

PROCEEDINGS

September 16 – 18, 2019

Lviv, Ukraine

ORGANIZERS:

- Ivan Franko National University of Lviv (Ukraine)
- IEEE Ukraine Section (Ukraine)
- IEEE Ukraine Section (West) MTT/ED/AP/EP/SSC Societies Joint Chapter (Ukraine)

PARTNERS:

- G. V. Karpenko Physico-Mechanical Institute of the NAS of Ukraine (Ukraine)
- Lviv Centre of Institute for Space Research of NAS of Ukraine and SSA of Ukraine (Ukraine)
- Lviv IT Cluster (Ukraine)
- Scientific Center of Polish Academy of Sciences in Kiev (Poland, Ukraine)
- Lublin University of Technology (Poland)
- Institute of Information Technology, Lodz University of Technology (Poland)
- University of Zielona Góra (Poland)
- Bohdan Dobrzański Institute of Agrophysics (Poland)

2019 XIth International Scientific and Practical Conference on Electronics and Information Technologies (ELIT)

Part Number CFP19LIT-ART

ISBN 978-1-7281-3561-8

Copyright and Reprint Permission: Abstracting is permitted with credit to the source. Libraries are permitted to photocopy beyond the limit of U.S. copyright law for private use of patrons those articles in this volume that carry a code at the bottom of the first page, provided the per-copy fee indicated in the code is paid through Copyright Clearance Center, 222 Rosewood Drive, Danvers, MA 01923. For reprint or republication permission, email to IEEE Copyrights Manager at pubs-permissions@ieee.org.

All rights reserved. Copyright ©2019 by IEEE

ORGANIZING COMMITTEE

Kukharskyy V., Dr., Lviv, Ukraine (Co-Chairman)
Sobczuk H., Prof., Kyiv, Ukraine (Co-Chairman)
Bolesta I., Prof., Lviv, Ukraine (Vice-Chairman)
Muravsky L., Prof., Lviv, Ukraine (Vice-Chairman)
Karbovnyk I., Dr., Lviv, Ukraine (Secretary)
Dzdzelyuk O., Lviv, Ukraine
Furgala Yu., Dr., Lviv, Ukraine
Kushnir O.S., Prof., Lviv, Ukraine
Kushnir O.O., Dr., Lviv, Ukraine
Melnyk M., Dr., Lviv, Ukraine
Monastyrskiy L., Dr., Lviv, Ukraine
Nazarkevych M., Dr., Lviv, Ukraine
Rovetsky I., Dr., Lviv, Ukraine
Rogowski J., Dr., Lodz, Poland
Shmygelsky Ya., Lviv, Ukraine
Shuwar R., Dr., Lviv, Ukraine

PROGRAMME COMMITTEE

Gladyshevskii R., Prof., Lviv, Ukraine (Chairman)
Andriychuk M., Prof., Lviv, Ukraine (Vice-Chairman)
Nazarchuk Z., Prof., Lviv, Ukraine (Vice-Chairman)
Velhosh S., Dr., Lviv, Ukraine (Secretary)
Alexandrov M., Prof., Barcelona, Spain
Buhrii O., Prof., Lviv, Ukraine
De Leo N., Dr., Turin, Italy
Dochviri J., Prof., Tbilisi, Georgia
Dyyak I., Dr., Lviv, Ukraine
Eglitis R., Dr., Riga, Latvia
Febvre P., Dr., Chambery, France
Fitio V., Prof., Lviv, Ukraine
Golovchak R., Prof., Clarksville, USA
Horabik J., Prof., Lublin, Poland
Hotra O., Prof., Lublin, Poland
Ilyenko K., Dr., Kharkiv, Ukraine
Kisala P., Prof., Lublin, Poland
Kovalenko O., Prof., Dnipro, Ukraine
Medikovsky M., Prof., Lviv, Ukraine
Mykhaylyk V., Prof., Didcot, UK
Ogirko I., Prof., Lviv, Ukraine
Padlyak B., Prof., Zielona Góra, Poland
Plecenik T., Dr., Bratislava, Slovakia
Popov A., Dr., Riga, Latvia
Rusyn B., Prof., Lviv, Ukraine
Sławiński C., Prof., Lublin, Poland
Stakhiv P., Prof., Lviv, Ukraine
Stepashko V., Prof., Kyiv, Ukraine
Teslyuk V., Prof., Lviv, Ukraine
Tsmots I., Prof., Lviv, Ukraine
Shynkarenko H., Prof., Lviv, Ukraine
Venherskyi P., Prof., Lviv, Ukraine
Vorobel R., Prof., Lviv, Ukraine
Wójcik W., Prof., Lublin, Poland
Yuzevych V., Prof., Lviv, Ukraine

TABLE OF CONTENTS

Information Technologies

Discrete-Time Control of Capacitated Multi-Channel Distribution Systems with Batch Replenishments <i>Przemysław Ignaciuk</i>	2
Detection of Subsurface Defects in Composite Panels Using Dynamic Speckle Patterns <i>Leonid Muravsky, Oleksandr Kuts, Georgiy Gaskevych, Olga Suriadova</i>	7
About Improving the Measuring Distances Accuracy Based on Correlation Analysis of Stereo Images <i>Vladimir Kozlov, Waldemar Wojcik, Natalia Zgirovskaya</i>	11
Biometric Identification System with Ateb-Gabor Filtering <i>Mariya Nazarkevych, Nataliia Lotoshynska, Vasyl Brytkovskyi, Serhii Dmytruk, Vasyl Dordiak, Iryna Pikh</i>	15
Comparison of the Effectiveness of Fingerprint Skeletal Methods <i>Mariya Nazarkevych, Vasyl Dordiak, Vasyl Brytkovskyi, Khrystyna Pelekh, Iryna Pikh, Yaroslav Voznyi</i>	19
Identification of Wear Products in the Automotive Tribotechnical System Using Computer Vision Methods, Artificial Intelligence and Big Data <i>Olexiy Balitskii, Valerii Kolesnikov</i>	24
Competence-Based Hierarchical Case Base for Control of Unmanned Vehicle Teams <i>Vladimir Sherstjuk, Nataliia Kozub, Igor Sokol, Ruslan Levkivskyi</i>	28
Development and Usage of a Computer Model of Evaluating the Scenarios of Projects for the Creation of Fire Fighting Systems of Rural Communities <i>Roman Ratushny, Anatolii Tryhuba, Oleg Bashynsky, Vadym Ptashnyk</i>	34
Development of Client and Server Software for use in Mass Service Facilities <i>Orest Babych, Yurii Hutak, Arthur Yuzkiv, Oleksandr Futey</i>	40
Conciseness of Ukrainian, Russian and English: Application to Translation Studies <i>Oleg Kushnir, Oksana Dzera, Liliya Kushnir</i>	44
Computational-Measurement System “Nanoplasmonics”. Part 1: Architecture <i>Ivan Bolesta, Oleksii Kushnir, Mykhailo Bavdys, Ivan Khvyshchun, Antonina Demchuk</i>	51
Computational-Measurement System “Nanoplasmonics”. Part 2: Structure of Microservices <i>Ivan Bolesta, Oleksii Kushnir, Mykhailo Bavdys, Ivan Khvyshchun, Antonina Demchuk</i>	55
Recognition of Handwritten Images Using Multilayer Neural Networks <i>Volodymyr Bihday, Volodymyr Brygilevych, Yurii Hychka, Zinovii Liubun, Nazar Pelypets, Vasyl Rabyk</i>	59
The Expert System “Pharmacy” for Determination of Availability and Conditions of Storage of Medicinal Products <i>Serhiy Sveleba, Ivan Kunyo, Nataliya Sveleba, Ivan Karpa, Ivan Katerynchuk</i>	63

Understanding the Basics of the Model-Based Techniques for Control Engineers with Simulink and BeagleBone Black: Processor-in-the-Loop Simulation of a DC Motor Speed Control <i>Oleksiy Kuznyetsov</i>	67
Oxygen Saturation Variability: Healthy Adults <i>Gennady Chuiko, Olga Dvornik, Yevhen Darnapuk, Yaroslav Krainyk</i>	72
Sliding Mode Interval Controller for the Mobile Robot <i>Roman Voliansky, Oleksandr Sadovoi, Yuliia Sokhina, Iurii Shramko, Nina Volianska</i>	76
Solution of Filtering and Extrapolation Problems when Constructing Recovery Control in Stochastic Differential Systems <i>Oleg Mashkov, Vadym Ptashnyk, Viktor Chumakevych</i>	82
The Concept of Machine Learning and Elliptic Curves United Approach in Solving of the Factorization Problem <i>George Vostrov, Ivan Dermenzhy</i>	87
Mathematical Modeling of Complex Dynamical Systems when Changing their Structure <i>Bohdan Melnyk, Nataliya Melnyk, Zoriana Melnyk</i>	92
Fractal Analysis of Porous Structures Using a Fuzzy Logic System <i>Igor Olenych, Yurii Olenych, Andriy Kostruba, Yaroslav Pryima</i>	97
Dynamic Processes of Formation Classes of Prime Numbers in a Probabilistic Model of Mathematical Computer Proof of the Generalized Artin Hypothesis <i>George Vostrov, Roman Opiata</i>	102
Using Artificial Neural Networks to Forecast Stock Market Indices <i>Svitlana Pryima, Roman Vovk, Volodymyr Vovk</i>	108
The Lyapunov's Exponents Variation on System with Incommensurate Superstructure Under Surface Energy Field <i>Serhiy Sveleba, Ivan Katerynychuk, Ivan Kunyo, Yaroslav Shmygelsky, Ivan Karpa</i>	113
Investigation of Geoinformation Models of Water Flows in Pseudoprismatic Channels <i>Yaryna Kokovska, Petro Venherskyi</i>	117
Monitoring the Virtual Reality Influence on Cognitive Tasks Performance in Healthy Individuals <i>Andrii Cholach, Solomiya Lebid</i>	121
Performance Analysis of Messages Queue in the Different Actor System Implementation <i>Baseem A. Al-Twajre</i>	127
Contactless IoT Sensor of Liquid Level based on Impedance Method <i>Bohdan Blagitko, Yuriy Mochulskyi, Ihor Zajachuk, Micle Batiuk, Ihor Kravets, Volodymyr Bihday</i>	132
Abstraction as a Way of Uncertainty Representation in Smart Rules Engine <i>Anatolii Kargin, Tetyana Petrenko</i>	136
An Improved Facial Recognition Technique Using Scale and Rotation Invariant Statistical Moments <i>Yaser Daanial Khan</i>	142
On Intelligent Decision Making in Multiagent Systems in Conditions of Uncertainty <i>Dmytro Chumachenko, Ievgen Menailov, Kseniia Bazilevych, Tetyana Chumachenko</i>	150
Neural Element of Parallel-Stream Type with Preliminary Formation of Group Partial Products <i>Ivan Tsmots, Vasyl Rabyk, Oleksa Skorokhoda, Taras Teslyuk</i>	154

On the Development of Object Detector Based on Capsule Neural Networks <i>Oleh Sinkevych, Daniil Berezhansky, Zenyk Matchyshyn</i>	159
Bitcoin Price Predictive Modeling Using Expert Correction <i>Bohdan Pavlyshenko</i>	163
Method of Neural Network Training with Integer Weights <i>Oleksandr Karpin, Vasyl Mandziy, Zinovii Liubun, Vasyl Rabyk</i>	168
Adaptive Iterative Pruning for Accelerating Deep Neural Networks <i>Yuri Gordienko, Yuriy Kochura, Vlad Taran, Nikita Gordienko, Andrii Bugaiov, Sergii Stirenko</i>	173
Normalization Modifications for Fast Self-Quotient Image Method <i>Vitalii Parubochyi, Roman Shuvar</i>	179
IoT Image Recognition System Implementation for Blind Peoples Using esp32, Mobile Phone and Convolutional Neural Network <i>Vasyl Kushnir, Bogdan Koman, Volodymyr Yuzevych</i>	183
Deep Learning for Atmospheric Cloud Image Segmentation <i>Bohdan Rusyn, Valentyna Korniy, Oleksiy Lutsyk, Rostyslav Kosarevych</i>	188
One-step Prediction of Air Pollution Control Parameters using Neural-Like Structure Based on Geometric Data Transformations <i>Oleksandra Mishchuk, Roman Tkachenko</i>	192
The Usage of Apache Spark for Collection and Analysis of Social Networking Statistics <i>Ihor Tovpinets, Roksolana Kovtko, Volodymyr Yuzevych, Andrii Prodyvus</i>	197

Computer Electronics

Prototype of Local Positioning System <i>Lyubomyr Monastyrskyi, Yaroslav Boyko, Danylo Maksymchuk</i>	202
Apparatus and Technique for Investigating the Effective Seismic Wave Velocity in the Sediment Layer Using the Refracted Wave Method <i>Yuri Datsyuk, Bogdan Kuplovskiy</i>	206
Configurable Description of FPGA-based Control System for Sensor Processing <i>Yaroslav Krainyk, Yevhen Darnapuk</i>	210
Information Technology of Surveys and Diagnostics of Underground Pipelines <i>Roman Dzhala, Vasyl' Dzhala, Bohdan Horon, Oleh Senyuk, Bohdan Verbenets'</i>	214
Specialized Device to Control Work of Executive Mechanism Using Operator's Hand Gestures <i>Oleksii Voronchuk, Halyna Klym, Roman Dunets</i>	218
Physical and Geological Factors in Modeling of the Climate Earth Changes <i>Vitaly Fourman</i>	222
Simulation of Energy Schemes and Electron Spectrum in Plane Nitride Semiconductor Nanostructures <i>Igor Boyko, Halyna Tsupryk, Iaroslav Kinakh, Yurii Stoianov</i>	227

Influence of Bi Impurity on the Electronic Structure and Photoelectric Properties of Germanium Monosulfide <i>Dmytro Bletskan, Vasyl Kabatcii</i>	232
Computer Calculation of Cation Migration Channels in Scheelite Structure <i>Volodymyr Shevchuk, Ihor Kayun</i>	238
Diffraction Analysis of Finite Cross-Section Light Beam on Grating with Normal Incidence <i>Volodymyr Fitio, Andriy Bendzyak, Iryna Yaremchuk, Yaroslav Bobitski</i>	242
Optical Properties and Band Structure of $\text{Cu}_7\text{SiS}_5\text{I}$ Crystal <i>Dmytro Bletskan, Ihor Studenyak, Vasyl Vakulchak</i>	247
Aluminum Nitride Thermal Interface for Improving Heat Performance of High-Power Electronic Devices <i>Eduard Rudenko, Ihor Korotash, Maxim Dyakin, Denis Polotsky, Mikhail Belogolovskii, Yuri Strzhemechny</i>	253
Ultra-Low Resistance in Carbon Nanostructures <i>Eduard Rudenko, Ihor Korotash, Anatolij Krakovny, Denis Polotsky, Mikhail Belogolovskii, Vitaliy Perepelytsia</i>	257
Investigating a Discrete Model of Memristive Systems <i>Kirill Ochkan, Sasan Razmkhah, Pascal Febvre, Elena Zhitlukhina, Mikhail Belogolovskii</i>	261
Synergetic Processes in Uniaxially Deformed Crystals <i>Bohdan Koman, Volodymyr Yuzevych</i>	265
Magnetodielectric Effect in a New Multiferroic Crystals of Tetraethylammonium Tetrahalogenocobaltate <i>Volodymyr Kapustianyk, Svitlana Semak, Pavlo Yonak, Bohdan Kundys, Yurii Chornii</i>	268
Birefringence of Tl_4HgI_6 Crystal <i>Andriy Kashuba, Mykola Solovyov, Taras Malyi, Ihor Semkiv, Andriy Franiv</i>	272
Low Temperature Luminescence of ZnWO_4 Crystals with Li Impurity <i>Stepan Novosad, Ludmyla Kostyk, Volodymyr Kapustyanyk, Iryna Novosad, Mykola Rudko, Myron Panasyuk</i>	277
Luminescence Properties of the Tm^{3+} -doped LiKB_4O_7 Glass <i>Bohdan Padlyak, Ihor Kindrat, Volodymyr Adamiv, Ihor Teslyuk</i>	280
Structure, Surface Morphology and Luminescence Properties of $\beta\text{-Ga}_2\text{O}_3$ and $(\text{Y}_{0.06}\text{Ga}_{0.94})_2\text{O}_3$ Thin Films <i>Oleh Bordun, Bohdan Bordun, Igor Kukharskyy, Ivanna Medvid</i>	285
Effect of Preparation Conditions and Impurities on the Spectral Characteristics of Cadmium Iodide <i>Iryna Novosad, Bogdana Kalivoshka, Stepan Novosad, Andriy Vas'kiv</i>	291
The Impact of Radiation Defects on a Photosensitivity of Silicon Single Crystals <i>Serhiy Luniov, Mykola Khvyshchun, Volodymyr Maslyuk</i>	295
Method for the Formation of a Diffraction Grating on the Semiconductors Surfaces <i>Halyna Petrovska, Iryna Yaremchuk, Serhiy Malynych, Yaroslav Bobitski</i>	299

Effect of Deep Trap Levels on Green Luminescence in β -Ga ₂ O ₃ <i>Vyacheslav Vasylytsiv, Andriy Luchechko, Lyudmyla Kostyk, Bohdan Pavlyk</i>	303
Structural Properties of Polycrystalline BaGa ₂ O ₄ Ceramics Doped with Eu ³⁺ Ions <i>Yuriy Kostiv, Andriy Luchechko, Halyna Klym, Ivan Karbovnyk, Bohdan Sadovyi, Oksana Zaremba, Oleh Kravets</i>	307
Transformation of Positron Trapping Parameters Caused by Water Molecules in Voids Near Grain Boundaries in MgAl ₂ O ₄ Ceramics <i>Halyna Klym, Adam Ingram, Roman Szatanik</i>	312
Temperature and Pressure Changes of the Refractive Properties of LiNH ₄ SO ₄ Crystal in β Modification <i>Myron Rudysh, Vasyl Stadnyk, Pavlo Shchepanskyi, Ruslan Brezvin, Oleg Kushnir, Galyna Myronchuk, Igor Matviishyn</i>	316

Information Technologies

- Information Systems
- Mathematical and Computer Modeling
- Internet of Things
- Artificial Intelligence Systems
- Data Science and Machine Learning
- High Productivity Computing Systems and Big Data

Influence of Bi Impurity on the Electronic Structure and Photoelectric Properties of Germanium Monosulfide

Dmytro Bletskan
 Faculty of Physics
 Uzhhorod National University
 Uzhhorod, Ukraine
 crystal_lab457@yahoo.com

Vasyl Kabatcii
 Faculty of Economics, Management
 and Engineering
 Mukachevo State University
 Mukachevo, Ukraine
 vm@msu.edu.ua

Abstract—Quantum-chemical studies of GeS electronic structure containing isolated substitutional impurities Bi_{Ge} and $\{\text{V}_{\text{Ge}}\text{-Bi}_{\text{Ge}}\}$ -type complexes were performed using density functional theory in the LDA+U-approximation as well as their role in the formation of photoelectric characteristics of the crystals was discussed. It was established that the localization of Bi impurity predominantly in the germanium positions induces the appearance of donor-type levels in the band gap compensating the acceptor levels formed by cation vacancies which leads to the increase of dark resistivity as well as the sharp increase of photosensitivity of GeS crystals.

The features of chemical bonding in the defect-free and defective GeS crystals were analyzed on the basis of electronic density distribution maps. Electronic density maps clearly show the covalent-ionic bond nature within the corrugated double-layer packets with the predominant charge concentration on Ge-S (Bi-S) bonds as well as the weak van der Waals bond components between double-layer packets with the participation of germanium electronic lone pair.

Keywords—germanium monosulfide, electronic structure, impurity defects, photoconductivity

I. INTRODUCTION

Great interest in layered crystals and thin layers of germanium monosulfide (GeS) is caused by the unique combination of their structure and physical properties that make them attractive to use as electric memory devices [1], as holographic recording media [2, 3], as photo-absorbing layers for the photovoltaic devices (solar cells) [4] as well as for the production of heterostructures by optical contact bonding [5], Schottky barriers [6], photoreceivers of linear polarized radiation [7], photoelectric sensors for the solar energy modules [8, 9], optoelectronic sensors [10]. Photoelectric receivers of linear polarized radiation require the strongly anisotropic crystals that meet a number of requirements for ensuring the optimal values of operating device parameters: high photosensitivity in the specified spectral range, dark- and photoresistance, intertance, operating temperature range, etc.

Typical feature for germanium monosulfide is the nonstoichiometry which appears as a result of crystal structure regularity violation due to the presence of intrinsic point defects [11].

The presence of large number of intrinsic point (zero-dimensional) defects in GeS layered crystals determines the concentration of free charge carriers and the lifetime of minor charge carriers, i.e. ultimately the efficiency of

optoelectronic devices created on their basis. Intrinsic defects, being electrically charged, form the p -type conductivity and high concentration (10^{17} – 10^{18} cm^{-3}) of charge carriers (holes), which makes these crystals as low-impedanced and slightly photosensitive.

The regulation of intrinsic point defects by donor impurity Bi doping is an effective way to modify the physical macroscopic properties of GeS layered crystals. The important information about the electronic characteristics of bismuth impurity atoms at their interaction with the electrons of a matrix can be obtained from the theoretical calculations of electronic structure and experimental studies of impurity states from photoconductivity spectra. It should be noted that by now the electronic structure of ideal defect-free stoichiometric GeS has been already studied using various band theory computational methods: semiempirical pseudopotential [12], linear combination of atomic orbitals (LCAO) [13], first-principle calculation method based on the density functional theory [14], Hartree-Fock and full-potential linearized augmented plane wave (FP-LAPW) methods [15]. Along with the theoretical studies, there are also experimental investigations of the features of GeS electronic states by the ultraviolet and X-ray photoelectron spectroscopy [16–23] as well as electron energy loss spectroscopy [24] methods.

This paper presents the quantum chemical investigation results of electronic structure for GeS crystals containing isolated substitutional impurity atoms Bi_{Ge} ($\text{Bi} \rightarrow \text{Ge}$) and also vacancy-impurity complexes $\{\text{V}_{\text{Ge}}\text{-Bi}_{\text{Ge}}\}$. It is discussed the role of these defects in the formation of photoconductivity spectral characteristics. The energy bands, total and partial densities of states appears as the calculation results. The charge density maps were used for the illustration of individual interatomic interactions.

II. CRYSTALS PREPARATION AND THEIR STRUCTURE

GeS:Bi crystals were grown in order to verify the consequences obtained as results of quantum-chemical modeling of electronic structure of bismuth doped germanium monosulfide. The doped crystals were obtained as follows: metallic bismuth in an amount 0.1 and 1.0 at. % was added into the initial furnace charge before synthesis start and the synthesis process was carried out together with the impurity. After synthesis finish the obtained polycrystalline ingot was shaken off into one ampoule end and then it has been placed in the horizontal two-zone

tubular furnace of resistive heating. The optimum crystal growth conditions are followed: the temperature of evaporation zone is 900 K; the temperature of condensation zone is 800 K. Crystals from the gas phase were grown in the form of plane-parallel plates with the dimensions up to $8 \times 15 \times 0.1$ mm. The layered structure character explains the lamellar habit of GeS:Bi crystals with well-developed faces (001).

Germanium monosulfide crystallizes in the orthorhombic structure with the lattice parameters $a = 4.299$ Å, $b = 3.646$ Å, $c = 10.481$ Å, $Z = 4$, its symmetry is described by D_{2h}^{16} ($Pcmn$) space group [25]. GeS structure is a derivative of black phosphorus structure, the half of atoms of its orthorhombic cell is replaced by Ge atoms and the second half by S atoms (Fig. 1, *a*).

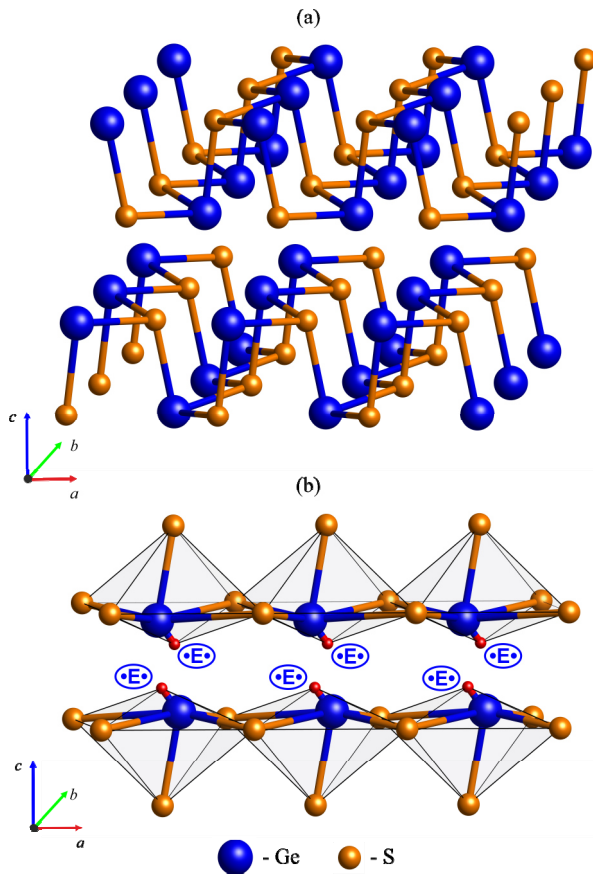


Fig. 1. Crystal structure (a) and ψ -octahedra $[\text{GeS}_5 \cdot \text{E} \cdot]$ packing (b) in the orthorhombic GeS phase ($\cdot \text{E} \cdot$ – electronic lone pair).

The electronic configurations of valence electrons for germanium and sulfur atoms are $3d^{10}4s^24p^2$ and $3s^23p^4$ respectively. Sulfur is a more electronegative element in GeS compound, so it takes two electrons from germanium atom, which leads to the electronic configuration $3s^23p^6$ for S^{2+} and $3d^{10}4s^24p^0$ for Ge^{2-} . Thus, the germanium oxidation state in GeS is equal II (2+). In this state, two $4p$ -electrons of germanium participate in the chemical bond formation while two $4s$ -electrons form the lone pair. This electronic lone pair is not directly involved in the chemical bond formation, but it significantly affects the asymmetrical arrangement of sulfur atoms around germanium atom that finally leads to the formation of distorted ψ -octahedra $[\text{GeS}_5 \cdot \text{E} \cdot]$, where $\cdot \text{E} \cdot$ is the electronic lone pair. These coordinating ψ -octahedra of Ge atoms are edge-connected to each other and form the corrugated double-layer packets in

the XY plane (Fig. 1, *b*). Double-layer packets are packed along the c axis and connected together by the weak van der Waals forces while the ionic-covalent bond type acts inside the double-layer packets.

III. CALCULATION METHOD

At the present time, the supercell model with the application of *ab initio* electronic structure calculation methods [26] is most effectively used for the description of electronic structure of defect crystals. We performed the electronic structure calculations in the framework of density functional theory using the basic sets of plane waves (PW), linearized combination of atomic orbitals (LCAO) and norm-conserving pseudopotentials, as realized in the SIESTA and ABINIT [27–30] software packets. It is well-known that the first-principle calculations within the density functional theory in the local density approximation (LDA) for the exchange-correlation potential give the underestimated value of the band gap width. The accounting of direct Coulomb single-site interaction U within the Hubbard model [31] can significantly affect the value of fundamental band gap width, the depth of defect states in the bandgap as well as the charge localization. Therefore, the LDA+ U -approximation in comparison with the LDA-calculations were used in the present work for a correct description of electronic correlations [32, 33].

The $2 \times 2 \times 1$ supercell was used in our calculations; it was obtained by the double translation of germanium monosulfide orthorhombic primitive cell along the directions of crystallographic a and b axes. The choice of such cell is optimal because it allows one to carry out a structural relaxation of nearest atoms without the essential increase of computation time. The supercell model using suggests the impurity ordering in the calculation whereas the disordering effects in the real-doped crystals significantly affect their photoelectric properties. Modeling of impurity in the supercell containing 32 atoms instead of one Ge atom, one Bi atom was introduced. The relaxation procedure of supercell geometry (preserving the overall crystal symmetry) was performed for each considered defect configurations to achieve the total energy minimum E_{tot} and the force values acting on the ions less than 0.01 eV/Å.

IV. RESULTS AND DISCUSSION

A. Electronic structure and density of states

The introduction of Bi impurity atoms into germanium monosulfide can significantly affect its electronic structure, conductivity, photoconductivity and other properties. This influence considerably depends on: 1) the position of introduced impurity atom in the matrix crystal lattice; 2) the natural atomic point defects which concentration considerably varies with the introduction of impurity atoms; 3) the association between the impurity atom and the intrinsic atomic point defects. We have considered two most probable variants of the introducing of Bi impurity atoms into GeS crystal matrix: the cation substitution (Bi atom in the cation positions Bi_{Ge}) and the formation of complexes of «cation vacancy – impurity atom» $\{\text{V}_{\text{Ge}}\text{-Bi}_{\text{Ge}}\}$ -type.

The prevailing mechanism of bismuth doping effect in GeS at low impurity concentration (≤ 0.1 at. %) is the filling of cation sublattice by Bi^+ ions. We will consider the total and partial densities of states (Fig. 2, *b*) for the analysis of

the changes of GeS:Bi electronic structure (Fig. 2, *a*) caused by the substitution effect in germanium sublattice (Bi→Ge). The energy positions as well as the widths of valence band and conduction band are almost not undergoing significant changes at the transition from the defect-free crystal to the doped one. Thus, Bi→Ge substitution does not change the semiconductive properties of the matrix: all binding states are occupied, the conduction band is empty, and the energy gap is slightly decreasing. The main feature of electronic structure of bismuth-doped germanium monosulfide is the appearance of new states in the valence band depth: one below S3s-band and other in the gap between occupied S3s- and Ge4s+S3p-bands. These states appear due to the interaction of Bi6s-orbitals with 3s-orbitals of the closest sulfur atoms. Fermi's level is placed near the conduction band bottom at Bi→Ge substitution. There is a donor level in the forbidden gap below the Fermi's level with a depth 0.32 eV below the conduction band bottom.

It is necessary to take into account the interaction between the introduced impurity defects with the intrinsic crystal point defects for the analysis of properties of GeS doped crystals. The increasing of concentration of electrically active bismuth impurity introduced into GeS

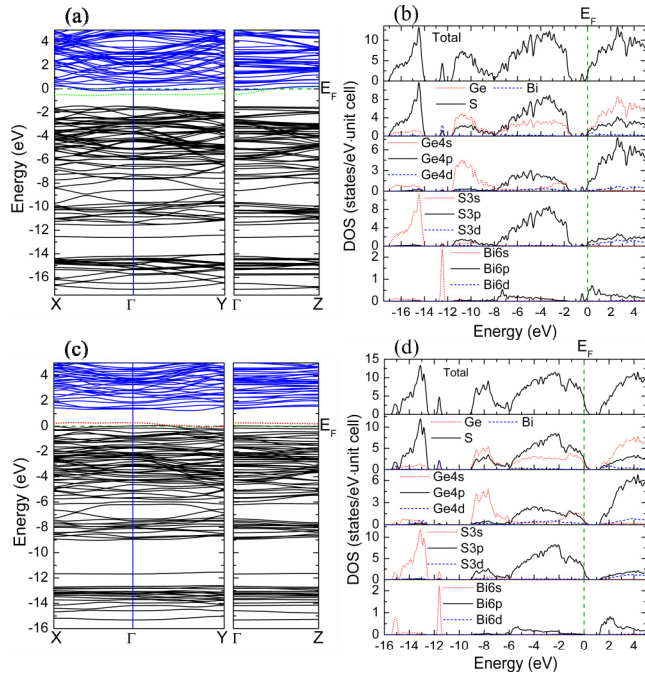


Fig. 2. Band structure, total and local partial density of states of GeS crystal with the cation substitutional impurity Bi_{Ge} (a, b) as well as with the $\{\text{V}_{\text{Ge}}-\text{Bi}_{\text{Ge}}\}$ defect type (c, d) in $2 \times 2 \times 1$ supercell model.

crystals leads to the increasing of solubility of intrinsic point defects of crystal lattice compensating the impurity doping effect that is the self-compensation phenomenon occurs. Along with the single cation vacancies, the formation of complexes consisting of impurity atoms and vacancies can significantly reduce the energy of defect formation and therefore it can significantly increase the self-compensation effect as well as to change the character of current carrier concentration dependence from the dopant content which ultimately affects the value of dark conductivity and impurity photoconductivity.

The changes of electronic structure at the simultaneous presence of two defect types, cation sublattice vacancies

(V_{Ge}) and substitutional defect of bismuth atom at germanium atom site (Bi_{Ge}) were considered for the supercell of $\text{Ge}_{0.875}\text{Bi}_{0.0625}\text{V}_{0.0625}\text{S}$ composition. Fig. 2, *c* and *d* present the electronic structure, total and partial densities of states for this $\{\text{V}_{\text{Ge}}-\text{Bi}_{\text{Ge}}\}$ complex configuration. The simultaneously presence of two types of lattice defects (structural vacancies and substitutional impurity $\{\text{V}_{\text{Ge}}-\text{Bi}_{\text{Ge}}\}$) in the germanium monosulfide crystal lattice causes the appearance in the gap between the occupied states of lowermost S3s-band and middle Ge4s+S3p-band two embedded states (Fig. 2, *c, d*), specific for the electronic structures with the presence of only V_{Ge} cation vacancy or only Bi_{Ge} substitutional impurity. The local impurity level of acceptor type with the depth $\Delta E_A = 0.1$ eV is formed in the band gap near the valence band top. Thus, the electronic structure modeling of germanium monosulfide with the presence of $\{\text{V}_{\text{Ge}}-\text{Bi}_{\text{Ge}}\}$ defect type should not lead to the conductivity type inversion which is confirmed experimentally.

B. Electronic density maps

The mechanism of chemical bonding formation in the defective germanium monosulfide can be analyzed in details by considering the electronic density contour maps constructed on the basis of DFT calculations in the supercell model. Figure 3 show the calculation results of valence electron charge density distribution of the GeS:Bi crystal in the form of electronic density maps for two characteristic crystallographic planes (001) and (010).

Interatomic interactions in the GeS have the combined character and include ionic, covalent and weak van der Waals components. From Fig. 3 *a* and *b* it can be seen that the charge density concentrates mainly within the corrugated double-layer packets. From the maps it is also visible that there are localized maxima on the Ge–S bonds which are combined together by the overall contours. A strongly pronounced deformation of contours $\rho(\mathbf{r})$ from sulfur atoms toward germanium atoms along the Ge–S bond line and the existence of the common contours encompassing the maxima of electron density over the cation-anion bonds (Fig. 3, *a* and *b*) characterize the covalent component of the chemical bond. The presence of the covalent bond component is caused by the hybridization of 4s-, 4p-states of germanium and 3p-states of sulfur (Fig. 2, *b*).

The ionic bond component is determined by the partial transfer of charge density from germanium atoms to sulfur atoms due to the difference of their electronegativities ($\text{EN}^{(\text{Ge})} = 2.01$, $\text{EN}^{(\text{S})} = 2.58$). Thus, electronic density maps are characterized by the higher valence electron density in the vicinity of sulfur sites.

Thus, the charge density in germanium monosulfide concentrates mainly within the corrugated two-layer packets while the electron density between packets is minimal which reflects the layered character of the crystal structure of this compound. The presence of an insignificant overlap of the wave functions related to the atoms of the nearest-neighbor double-layer packets is caused by the states of electronic lone pair ($\bullet\text{E}\bullet$) of germanium directed toward the interlayer van der Waals gap (Fig. 1, *b*).

Since the electronic density maps of crystals show the change of electron distribution at the formation of chemical

bonds between the matrix atoms (base substance) and impurity atoms, so they can serve as an evident illustration

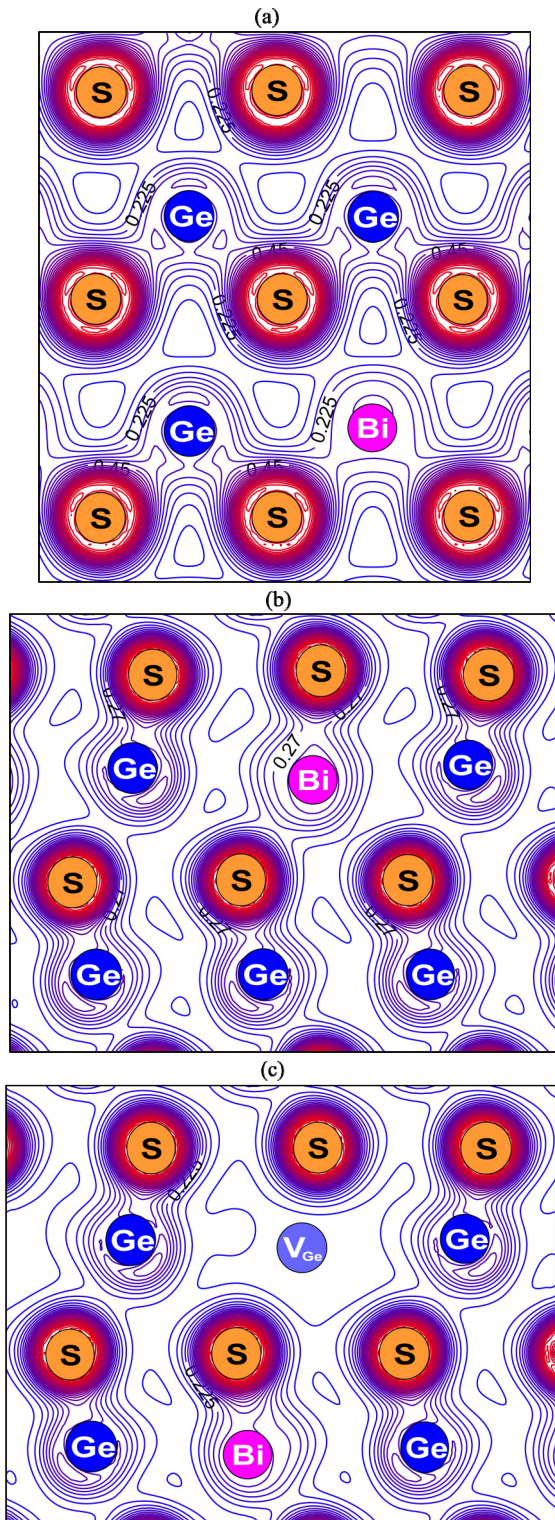


Fig. 3. Spatial distribution maps of valence charge density for GeS crystal with Bi_{Ge} substitutional impurity (a, b) and with a complex of $\{\text{V}_{\text{Ge}}\text{-Bi}_{\text{Ge}}\}$ -type in (001) (a) and (010) (b, c) planes.

of individual interatomic interactions. As it was mentioned in Sec A, the doping of GeS cation sublattice by Bi impurity leads to appear the fairly deep levels in the matrix electronic structure which correspond to the electronic states localized on bismuth atom and nearest sulfur atoms. It testifies the

occurrence of strong chemical bonding between bismuth and sulfur atoms. It is possible to establish the nature of these bonds by electronic charge spatial distribution analysis. The contours $\rho(\mathbf{r})$ between bismuth impurity and sulfur atoms (Fig. 3) are similar to the contours of cation and anion in the main matrix that testifies the strong chemical interaction between metal impurity atom and chalcogen atoms. The contours $\rho(\mathbf{r})$ near Bi impurity (Fig. 3) indicate the existence of covalent bonding component in the Bi-S bonds. The main role of covalent bonding between bismuth impurity and nearest sulfur atoms plays $\text{S}3p\text{-Bi}6p$ interaction.

C. Photoconductivity spectra of GeS:Bi crystals

For measurements of dark conductivity and photoconductivity, the coplanar contacts by indium fusing or aquadag coating were deposited on (001) natural crystal faces, so that electric field was applied along the crystallographic b axis. The ohmic character of contacts was confirmed by linearity of the VAC both under light as well as in the dark. According to the thermo-EMF sign it is found that both intentionally undoped and bismuth doped GeS crystals had p -type conductivity.

Doping of germanium monosulfide by Bi donor impurity within the solubility region leads to the significant increase of the specific dark resistivity ($\rho_t = 10^6\text{-}10^7$ Ohm-cm), thus it is not observed the inversion of conductivity type and the crystals are p -type conductivity. The self-compensation of donors by intrinsic defects (Ge vacancies) in GeS:Bi crystals at small impurity concentration is observed; it conclude that the formation of intrinsic lattice defects that gives the charge carriers of opposite sign at the introduction of electrically active Bi impurity into the crystal becomes energetically favorable. At the same time, the self-compensation of electrically active impact of Bi impurity in germanium monosulfide by single cation vacancies is insufficiently strong to explain the observed experimental regularities, in particular, the absence of conductivity sign inversion. The part of impurity ions becomes bind into the complexes with cation vacancies on bismuth concentration increase. The formation of complexes consisting of impurity atoms and vacancies along with the single vacancies can significantly reduce the energy of defects and thus considerably increase the self-compensation effect as well as change the character of dependence of the charge carrier concentration on the dopant impurity content. If consider that the bismuth impurity atoms are singly ionized Bi^- and the cation vacancies in GeS are doubly charged $\text{V}_{\text{Ge}}^{++}$, then the pairwise complexes $\{\text{V}_{\text{Ge}}\text{-Bi}\}$ are positively charged creating one charge carrier (hole) per one complex, wherewith the absence of conductivity type inversion is conditioned.

The introduction of Bi impurity atoms into germanium monosulfide leads to appearance of high photosensitivity in the visible and near infrared spectral ranges along with the increase of specific dark resistivity. The photosensitivity of bismuth doped GeS crystals is by several orders of magnitude higher than the photosensitivity of intentionally undoped low-resistance crystals. So, the multiplicity of changes $\rho_{\text{dark}}/\rho_{\text{light}} = 10^3$ at 293 K and it reaches $\rho_{\text{dark}}/\rho_{\text{light}} = 10^4\text{-}10^5$ at low temperatures and illumination 10^4 lux.

The stationary photoconductivity spectra of high-resistance GeS crystals with different Bi impurity concentration are presented in Fig. 4 and 5. The PC spectra of slightly doped GeS crystals in addition to the intrinsic band-band maxima shows the impurity band with a maximum 1.34 eV and weak feature near intrinsic absorption edge with a maximum at 1.5 eV in $E||a$ polarization (Fig. 4). There are observed the well-resolved maxima in the intrinsic absorption edge region of intentionally undoped GeS crystals while in this spectral region of heavily doped compensated GeS:Bi crystals (~1 at. % of impurity) it appears a wide continuum, the impurity band is broadened, its intensity increases and the energy position of its maximum is shifted to the lower energy region 1.3 eV.

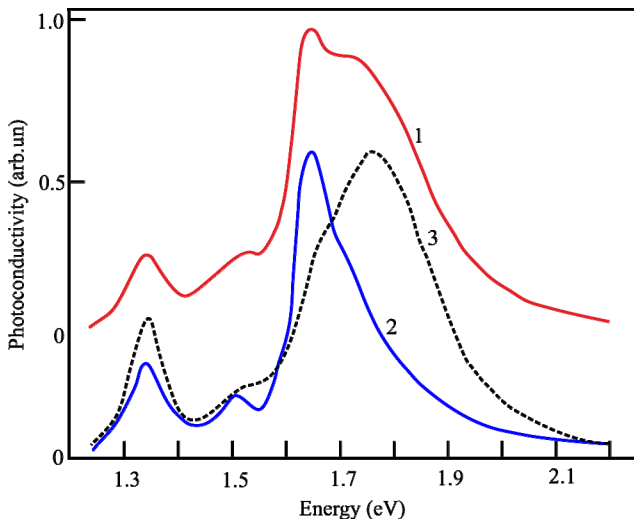


Fig. 4. Unpolarized (1) and polarized (2, 3) photoconductivity spectra of GeS:Bi crystal (0.1 atomic % of Bi): 2 – $E||a$; 3 – $E||b$; T = 293 K.

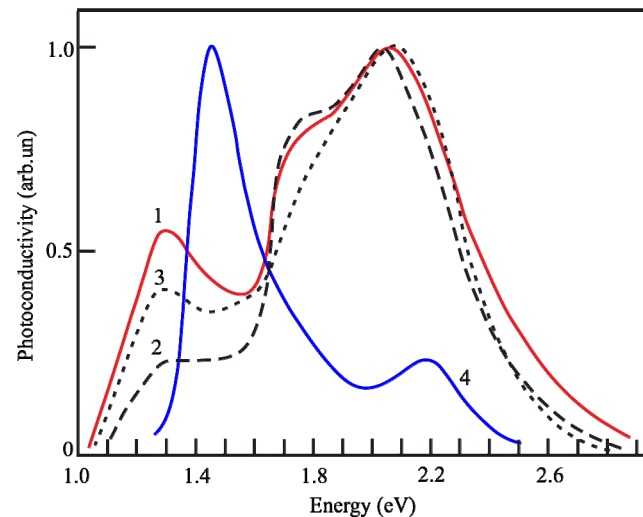


Fig. 5. Unpolarized (1, 4) and polarized (2, 3) photoconductivity spectra of GeS:Bi crystal (1 atomic % of Bi): 2 – $E||a$; 3 – $E||b$; T: 1, 2, 3 – 293 K; 4 – 90 K.

The change of character of spectral dependence of photosensitivity from the concentration of introduced Bi impurity into germanium monosulfide is naturally to associate with the change in the character of dissolution of impurity atoms in the matrix by increasing of their contents. As already noted above, the main mechanism of Bi impurity

dissolution in GeS for the slightly doped crystals is filling the cation vacancies. At the filling of cation vacancies by impurity atoms in GeS crystal lattice in addition to vacancies the new type of defects appears – substitutional impurity defects which similar to vacancies lead to the formation of donor level in the band gap (Fig. 2). The presence of impurity bands in PC spectrum with maxima at 1.34 and 1.5 eV is the confirmation of simultaneous presence in the band gap of donor level created by bismuth impurity and acceptor level formed by the charged cation vacancies respectively (curve 2, Fig. 4). The estimation of donor level depth created by Bi impurity as the difference between the energies of intrinsic ($h\nu_{int} = 1.65$ eV) and impurity ($h\nu_{imp} = 1.34$ eV) maxima in the PC spectra give us the value 0.31 eV which is close to the theoretically calculated 0.32 eV.

The heavily doped compensated GeS:Bi semiconductor is an example of disordered system because the chaotically located charged donors and acceptors create the large-scale fluctuations of electrostatic potential leading to the modulation of conduction band bottom and valence band top. Besides, the introduction of bismuth impurity atoms into GeS crystal lattice leads to the appearance of elastic stress fields caused by the difference of ionic atom radii of Ge^{2+} (0.73 Å) and Bi^{3+} (1.03 Å), and they can be easily amplified by inhomogeneous distribution of impurities. The presence of potential relief leads to the significant transformation of photoconductivity spectra both in the intrinsic and impurity regions (Fig. 5). The broadening and shift of intrinsic bands in the PC spectra to the lower energy region with the increasing of doping level of germanium monosulfide by bismuth can be qualitatively explained by a local decrease of band gap width due to "asymmetrical" curvature of conduction band and valence band at heavy doping.

Thus, the doping of germanium monosulfide by bismuth accompanied by the manifestation of a number of competing factors among which the next should be highlighted: the change in concentration of intrinsic cation vacancies (electroactive ones), the possibility of chemical interaction with the formation of complexes and the formation of fields of elastic distortions around the substitutional atoms.

The usage of supercell approach allows to calculate the electronic spectrum of germanium monosulfide both with a single impurity atom or with the high concentration of orderly located Bi impurity atoms. The calculation of electronic spectrum of Bi doped GeS with arbitrary impurity concentration and arbitrary function of their spatial distribution in the lattice is currently complicated. Thus, as the possibilities to calculate of electronic spectra of heavily doped compounds currently are rather limited, then the experimental methods sensitive to the restructuring of electronic spectra of heavily doped semiconductors in comparison with the defect-free ones are stepped forward. As it follows from the presented results, the spectral distribution of photoconductivity rightfully belongs to the number of such experimental methods.

V. CONCLUSIONS

Performed in this paper study based on the density functional theory allowed to determine the character of change of GeS band structure at the introduction of

substitutional impurity (Bi→Ge) and at the formation of complexes $\{V_{Ge}+Bi_{Ge}\}$. It was established that the Coulomb interaction account (LDA+*U*-approximation) significantly affects the band gap width and the depth of defect states in the comparison with the standard LDA-approximation.

It was performed the identification of observed features in the PC spectra of GeS:Bi crystals grown by the sublimation method based on the electronic structure calculation results. Substitutional Bi_{Ge} impurity with donor properties has the compensating effect on the intrinsic acceptor centers (V_{Ge}), causing the decreasing of concentration of free charge carriers (holes), and, as a result, it leads to the sharp increase of dark resistivity of GeS:Bi crystals without changing their conductivity type. Besides, Bi_{Ge} impurity substitutional atoms take a role of "sensitive" slow recombination centers responsible for the high integrated photosensitivity of doped crystals.

REFERENCES

- [1] D.I. Bletskan, V.I. Taran, and M.Yu. Sichka, "Switching effect in layer-like $A^{IV}B^{VI}$ crystals," *Ukrain. Phys. J.*, vol. 21, pp. 1436–1441, 1976.
- [2] P.P. Pogoretsky, E.N. Salkova, M.S. Soskin, D.I. Bletskan, and I.F. Kopinets, "Semiconductor material for hologram recording," USSR author's certificate, no 453976, 1974.
- [3] D.I. Bletskan, I.F. Kopinets, P.P. Pohoretsky, E.N. Salkova, and D.V. Chepur, "Production of GeS single crystals, investigation of their morphology and of latter influence on the hologram recording," *Kristallograf.*, vol. 20, pp. 1008–1012, 1975.
- [4] P.D. Antunez, J.J. Buckley, and R.L. Brutchey, "Tin and germanium monochalcogenide IV–VI semiconductor nanocrystals for use in solar cells," *Nanoscale*, vol. 3, pp. 2399–2411, 2011.
- [5] D.I. Bletskan, V.M. Kabatsii, Y.Y. Madyar, and T.A. Sakal, "Heterojunctions based on SnS_2 and GeS(Se) layered semiconductors," *Proceedings of IV International scientific-practical conference "Modern information and electronic technologies"*, p. 276, 2003.
- [6] C. Clemen, X.I. Saldaña, P. Munz, and E. Bucher, "Photovoltaic properties of some semiconducting layer structures," *Phys. Stat. Solidi (a)*, vol. 49, pp. 437–443, 1978.
- [7] D.I. Bletskan, N.V. Polazhinets, and D.V. Chepur, "Polarized investigation of photoconductivity of GeS_xSe_{1-x} single crystals," *Fiz. Tekh. Poluprovodn.*, vol. 17, pp. 1270–1274, 1983.
- [8] D.I. Bletskan and V.M. Kabatsii, "Photoelectric sensor for a solar power module," Patent of Ukraine, Bul. 14, no 106143, pp. 1-7, 2014.
- [9] D.I. Bletskan, V.M. Kabatsii, and M.M. Bletskan, "Photovoltaic sensor for the solar battery guidance on the sun based on GeS:Sb layered crystals," *Open Journal of Inorganic Non-Metallic Materials*, vol. 6, pp. 7–11, 2016.
- [10] D.I. Bletskan and V.M. Kabatsii, "Optoelectronic sensor," Patent of Ukraine, Bul. 12, no 105856, pp. 1-9, 2014.
- [11] D.I. Bletskan, *Crystalline and glassy chalcogenides of Si, Ge, Sn and alloys on their base*, vol. 1, Uzhhorod: Zakarpattia, pp. 292, 2004.
- [12] T. Grandke and L. Ley, "Angular-resolved uv photoemission and the band structure of GeS," *Phys. Rev. B*, vol. 16, pp. 832–842, 1977.
- [13] F.M. Gashimzade, D.G. Guliev, D.A. Guseinova, and V.Y. Shteinshrayber, "Band-structure calculation for A^4B^6 layered crystals by the equivalent-orbital linear combination of atomic orbitals method," *J. Phys.: Condens. Matter.*, vol. 4, pp. 1081–1091, 1992.
- [14] L. Makinistian and E.A. Albanesi, "First-principles calculations of the band gap and optical properties of germanium sulphide," *Phys. Rev. B*, vol. 74, pp. 045206-1–16, 2006.
- [15] Rathor, V. Sharma, N.L. Heda, Y. Sharma, and B.L. Ahuja, "Compton profiles and band structure calculations of IV–VI layered compounds GeS and GeSe," *Rad. Phys. Chem.*, vol. 77, pp. 391–400, 2008.
- [16] P.C. Kemeny, J. Azoulay, M. Cardona, and L. Ley, "Photoelectron spectra of GeS, GeSe, SnS and SnSe and their relation to structural trends and phase transitions within the average-valence – <5> compounds," *Nuovo Cimento B*, vol. 39, pp. 709–714, 1977.
- [17] Kosakov, H. Neumann, and G. Leonhardt, "Investigation of the band structure of germanium chalcogenides by means of photoelectron spectroscopy," *J. Electr. Spectr. Relat. Phenom.*, vol. 12, pp. 181–189, 1977.
- [18] H. Neuman and A. Kosakov, "Tight-binding calculation of the density of valence states of GeS, GeSe and GeTe," *Acta Phys. Polonica A*, vol. 55, pp. 779–784, 1979.
- [19] R.B. Shalvoy, G.B. Fisher, and P.J. Stiles, "X-ray photoemission studies of the valence bands of nine IV–VI compounds," *Phys. Rev. B*, vol. 15, pp. 2021–2024, 1977.
- [20] R.B. Shalvoy, G.B. Fisher, and P.J. Stiles, "Bond ionicity and structural stability of some average-valence-five materials studied by X-ray photoemission," *Phys. Rev. B*, vol. 15, pp. 1680–1697, 1977.
- [21] G.D. Davis, P.E. Viljoen, and M.G. Lagally, "Comparison of site-specific valence band densities of states determined from Auger spectra and XPS-determined valence band structure in GeS (001) and GeSe (001)," *J. Electr. Spectr. Relat. Phenom.*, vol. 21, pp. 135–152, 1980.
- [22] T. Chassé, U. Berg, and O. Brümmer, "Photoelectron diffraction and band structure effects in ARXPS from the valence bands of GeS," *Phys. Stat. Sol. (b)*, vol.132, pp. 141–144, 1985.
- [23] M. Taniguchi, R.L. Johnson, J. Ghijsen, and M. Cardona, "Core excitons and conduction-band structures in orthorhombic GeS, GeSe, SnS, and SnSe single crystals," *Phys. Rev. B*, vol. 42, pp. 3634–3643, 1990.
- [24] R. Eymard and A. Otto, "Optical and electron-energy-loss spectroscopy of GeS, GeSe, SnS and SnSe single crystals," *Phys. Rev. B*, vol. 16, pp. 1616–1623, 1977.
- [25] H. Wiedemeier and H.G. Schnering, "Refinement of the structures of GeS, GeSe, SnS and SnSe," *Z. Kristallogr.*, vol. 148, pp. 295–303, 1978.
- [26] R.A. Evarestov, *Quantum chemistry of Solids. LCAO Treatment of Crystals and Nanostructures*, 2nd ed., Springer-Verlag Berlin Heidelberg, pp. 734, 2012.
- [27] ABINIT. [Online]. Available : <http://www.abinit.org/>
- [28] X. Gonze, J.-M. Beuken, R. Caracas, F. Detraux, M. Fuchs, G.-M. Rignanese, L. Sindic, G. Verstraete, G. Zerah, F. Jollet, M. Torrent, A. Roy, M. Mikami, Ph. Ghosez, J.-Y. Raty, and D.C. Allan, "First-principle computation of material properties: the ABINIT software project," *Comp. Mat. Sci. B*, vol. 25, pp. 478–492, 2002.
- [29] SIESTA.[Online]. Available: <http://departments.icmab.es/leem/siesta/>
- [30] J.M. Soler, E. Artacho, J.D. Gale, A. Garcia, J. Junquera, P. Ordejón, and D. Sánchez-Portal, "The SIESTA method for ab initio order-N materials simulation," *J. Phys.: Condens. Matter.*, vol. 14, pp. 2745–2779, 2002.
- [31] J. Hubbard, "Electron correlations in narrow energy bands," *Proc. R. Soc. London. Ser. A.*, vol. 276, pp. 238–257, 1963.
- [32] V.I. Anisimov, J. Zaanen, and O.K. Andersen, "Band theory and Mott insulators: Hubbard U instead of Stoner I," *Phys. Rev. B*, vol. 44, pp. 943–954, 1991.
- [33] V.I. Anisimov, F. Aryasetiawan, and A.I. Lichtenstein, "First-principal calculations of the electronic structure and spectra of strongly correlated systems: the LDA+U method," *J. Phys.*, vol. 9, pp. 767–808, 1997.



МУКАЧІВСЬКИЙ ДЕРЖАВНИЙ УНІВЕРСИТЕТ

89600, м. Мукачево, вул. Ужгородська, 26

тел./факс +380-3131-21109

Веб-сайт університету: www.msu.edu.ua

E-mail: info@msu.edu.ua, pr@mail.msu.edu.ua

Веб-сайт Інституційного репозитарію Наукової бібліотеки МДУ: <http://dspace.msu.edu.ua:8080>

Веб-сайт Наукової бібліотеки МДУ: <http://msu.edu.ua/library/>